Journal of Inclusion Phenomena and Macrocyclic Chemistry
https://doi.org/10.1007/s10847-021-01082-6

ORIGINAL ARTICLE

3,5-Dibromophenyl-functionalised imidazolium salts and their corresponding $[Au(NHC)_2]^+$ complexes: synthesis, supramolecular chemistry and anti-cancer activity

Hawraa S. Al-Buthabhak[1,3] · Yu Yu[2,4] · Alexandre Sobolev[3] · Hani Al-Salami[5] · Murray V. Baker[3]

Received: 31 March 2021 / Accepted: 18 May 2021

Abstract
The synthesis and spectroscopic and structural characterisation of new 3,5-dibromophenyl-functionalised imidazolium salts and their corresponding $[Au(NHC)_2]^+$ complexes is reported. X-ray diffraction studies revealed intra- and intermolecular interactions involving the 3,5-dibromophenyl group, including Br…π interactions with imidazolyl and C_6 arene rings. Au-NHC complexes functionalised with 3,5-dibromophenyl substituents showed potent activity against OVCAR-8 (ovarian cancer) cells at low micromolar concentrations.

Keywords 3,5-Dibromophenyl-functionalised compounds · Imidazolium salts · Au-NHC complexes · Anti-cancer activity · Lipophilic cations · X-ray structures · Supramolecular Br…π interactions

Introduction

Mitochondria play a central role in regulating programmed cell death via apoptosis. Many cancers arise due to failures in mediating the apoptotic processes, resulting in ability to resist cell death and unrestricted proliferation of cancer cells [1–3]. Consequently, many cancer treatments target mitochondria as a way to promote apoptosis of cancer cells. Various cationic compounds, such as delocalised lipophilic cations (DLCs) [4–6] and cationic gold-phosphine complexes [7] and gold-NHC complexes, can accumulate in the mitochondria and subsequently trigger apoptosis [8].

Gold-based compounds, e.g., cationic gold-phosphine complexes [7, 9–12] and gold-NHC complexes, [8, 13, 14] are receiving much attention due to their promising anti-cancer activity against a wide variety of cancer cell lines [4, 15, 16]. The dominant proposed mechanism for the activity of Au-NHCs is that Au inhibits the activity of mitochondrial thioredoxin reductase (TrxR) by binding to the soft Se and S atoms in the cysteine and selenocysteine residues at the active site [4, 8]. TrxR is an important enzyme that regulates the cellular redox system and inhibition of TrxR can lead to a build-up of reactive oxygen species, which sets off a cascade of processes that leads to apoptosis [4, 16, 17].

The activity of Au-based compounds is highly dependent on their lipophilicity, with an increase in lipophilicity generally resulting in higher activity [4, 10]. Au complexes that behave as delocalised lipophilic cations can target TrxR in mitochondria. Since the mitochondrial membrane potential is higher (more negative) in cancer cells compared to normal cells, lipophilic, cationic Au-NHCs can selectively target mitochondria in cancer cells over normal cells [4]. However, for complexes that are too lipophilic, such as $[Au(dppe)_2]^+$ (dppe = 1,2-bis(diphenylphosphino)ethane), there can be severe toxic effects, such as cardiotoxicity [18] and hepatotoxicity [4]. Understanding the role of lipophilicity and

✉ Murray V. Baker
murray.baker@uwa.edu.au

Hawraa S. Al-Buthabhak
hawraas.dawood@uokufa.edu.iq

1 Department of Chemistry, Faculty of Science, University of Kufa, P.O. Box 21, Najaf 54001, Iraq

2 Curtin Medical School, Curtin Health Innovation Research Institute, Curtin University, Perth, WA 6102, Australia

3 School of Molecular Sciences M310, The University of Western Australia, 35 Stirling Highway, Perth, WA 6009, Australia

4 Division of Obstetrics & Gynaecology, The University of Western Australia Medical School, Perth, WA 6009, Australia

5 Biotechnology and Drug Development Research Laboratory, Curtin Medical School, Curtin Health Innovation Research Institute, Curtin University, Perth, WA 6102, Australia

Published online: 24 June 2021

structure–activity relationships of Au-NHC complexes is essential for enhancing their anticancer activity and minimising their undesirable side effects.

To date, while there is much evidence that Au-NHC complexes target mitochondria and trigger apoptosis, few studies have clearly shown subcellular distribution of Au-NHCs. One study of fluorescent dinuclear Au-NHCs by confocal fluorescence microscopy showed that these compounds were accumulated in lysosomes, not mitochondria [19]. Another study (by transmission electron microscopy) showed that when MDA-MB-231 human breast adenocarcinoma cells were incubated with $[Au(d2pype)_2]Cl$ (d2pype = 1,2-bis(2-pyridylphosphinoethane), electron rich elements (assumed to be Au) were accumulated in mitochondria [11]. The same study also showed (by NanoSIMS) that Au became associated with sulfur rich regions of the nucleus and cytoplasm of the cells [11]. Nevertheless, clear evidence concerning the fate of Au-NHC complexes and the NHC ligands themselves in cells remains elusive.

With the above considerations in mind, this work focuses on Au-NHC complexes containing 3,5-dibromophenyl substituents. These compounds are of interest for a number of reasons. Firstly, the 3,5-dibromophenyl substituents are large, lipophilic groups, and their inclusion in Au-NHC complexes introduces a new moiety that can be used to fine-tune lipophilicity and, hopefully, enhance biological activity. Secondly, halogens, and bromine in particular, can play a significant role in the activity of a drug due to the ability of halogens to participate in binding interactions with target molecules [20]. Thirdly, the 3,5-dibromophenyl substituents are a convenient moiety via which bromine atoms can be introduced into an NHC ligand and its Au-NHC complexes. Bromine atoms are convenient atomic labels that can be exploited in cellular mapping studies by the NanoSIMS technique.

In this study, Au-NHC complexes have been tested against OVCAR-8 ovarian cancer cells, a cisplatin-resistant cell line [21]. Previous genetic profiling on OVCAR-8 suggested that it resembles high-grade serous ovarian carcinoma in patients [22] which is the most common histological subtype of ovarian cancer.

Results and discussion

Synthesis and NMR studies

N-Arylation of heterocyclic compounds is typically achieved via an Ullman-type coupling of the heterocyclic compound with an aryl halide in the presence of a copper species as catalyst [23]. *N*-Phenylimidazole has previously been synthesized by reaction with iodobenzene in H_2O in presence of cuprous oxide, tetrabutylammonium bromide (as a phase transfer catalyst), and potassium phosphate at 130 °C [24]. Using a modification of this method (NaOH as base, DMSO as solvent, and no phase transfer catalyst), imidazole was *N*-arylated with bromobenzene and 1,3,5-tribromobenzene to form 1-phenylimdazole **1** and 1-(3,5-dibromophenyl)imidazole **2** respectively (Scheme 1). Subsequent *N*-alkylation resulted in the phenylimidazolium salt **3** and the 3,5-dibromophenylimidazolium salts **4**–**7**, and the hexafluorophosphate salt **8** was prepared by metathesis of the iodide salt **4** with KPF_6 (Scheme 1).

The new imidazolium salts **3** and **5**–**8** were converted into the corresponding complexes of form $[Au(NHC)_2]X$ (**9**–**13**) by reaction with (DMS)AuCl or (DMS)AuBr in the presence of K_2CO_3 at room temperature for 24 h (Scheme 1). The method used was a modification of the procedure reported by Collado et al., for the synthesis of other Au-NHC complexes [25]. The new complexes are soluble in a most organic solvent but not soluble in hexane or water.

Results of ^1H and ^{13}C NMR studies of the new salts **3**–**8** and complexes **9**–**13** are consistent with their proposed structures. During synthesis of the imidazolium salts **3**–**7**, formation of the imidazolium species was indicated by the appearance of ^1H NMR signals due to the azolyl H2 protons in the range 9.8–10 ppm and disappearance of the signal due to the H2 protons (~ 7.9 ppm) of the imidazole precursors **1** and **2**. In the $^{13}C\{^1H\}$ NMR spectrum, the signal due to the C2 carbon for the imidazolium salts **3**–**7** occurred near δ 137 ppm, which is consistent with the literature values for C2 in other imidazolium salts [8, 26, 27]. For the $[Au(NHC)_2]X$ complexes **9**–**13**, the $^{13}C\{^1H\}$ NMR spectrum showed a signal for the carbene carbon near 181 ppm, which is in the range reported for similar $[Au(NHC)_2]X$ [8, 28, 29].

X-ray studies

The new imidazolium salts **4**, **5**, and **8** and their complexes **10**–**13** have been characterised by X-ray diffraction. Details of solvents used in growth of crystals suitable for X-ray diffraction are recorded in the Experimental Section. Compounds **10** and **11** were obtained as the solvates **10**·EtOAc and **11**·CH_3CN. X-ray data and key bond lengths and angles summarised in Tables 1 and 2 respectively. The bond distances and angles are similar to corresponding values reported previously for similar imidazolium salts and Au-NHC complexes. Interesting features of the structures are summarised below.

The solid-state structure of 1-(3,5-dibromophenyl)-3-methylimidazolium iodide **4** contained two independent molecules (Fig. 1a). Interestingly, the 3,5-dibromophenyl moieties of the two molecules are approximately parallel and appear to be involved in a π–π interaction [30] (or Br-π interactions). The distance between the centroids of the C_6 rings is 4.70 Å and the distances between the centroid of

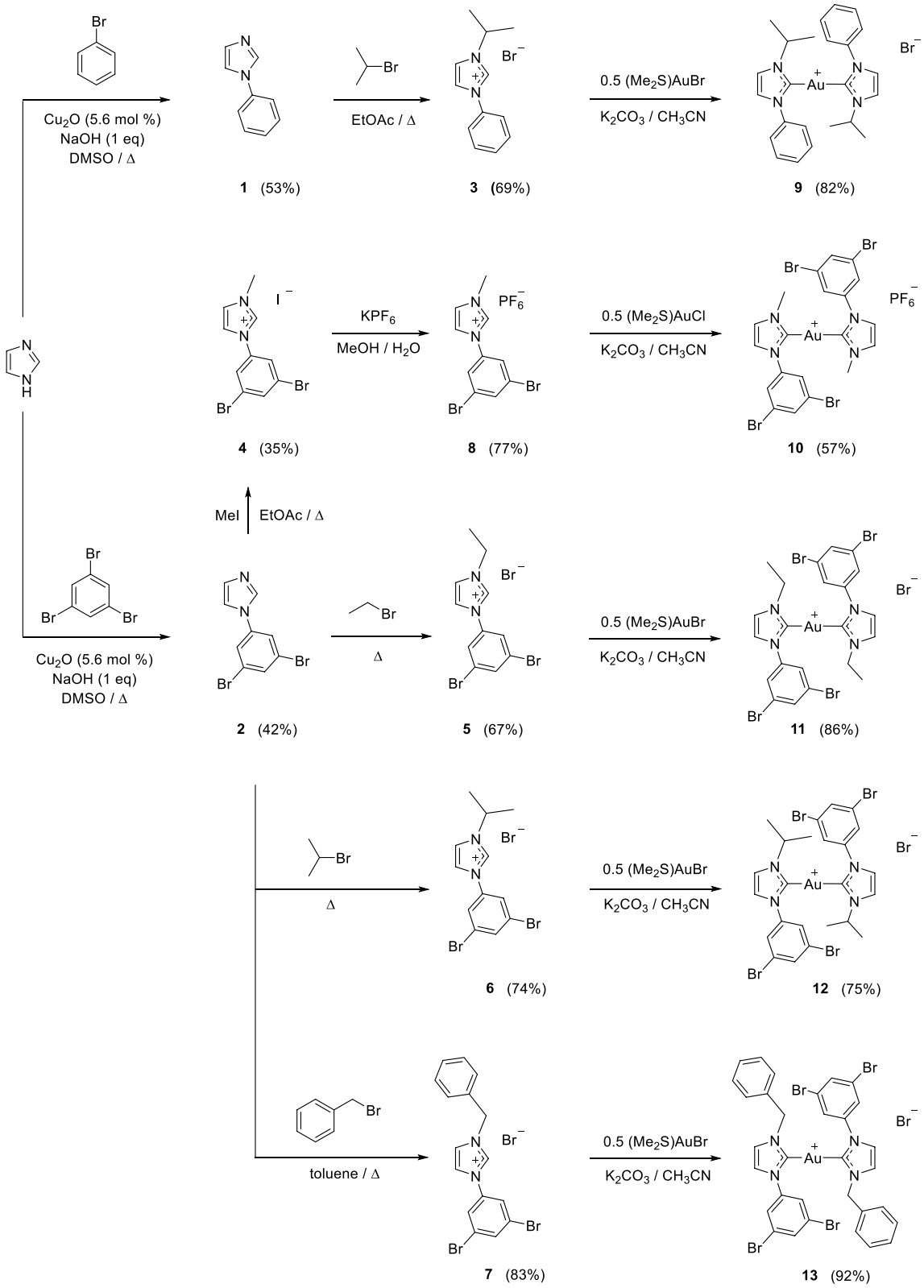

Scheme 1 Synthesis of *N*-arylimidazoles **1** and **2**, imidazolium salts **3–8**, and Au-NHC complexes **9–13**

Table 1 Crystal data for salts **4**, **5**, and **8** and complexes **10**–**13**

	4	**5**	**8**	**10**	**11**	**12**	**13**
Empirical formula	$C_{10}H_9Br_2N_2{\cdot}I$	$C_{11}H_{11}Br_3N_2$	$C_{10}H_9Br_2N_2{\cdot}F_6P$	$C_{20}H_{16}AuBr_4N_4{\cdot}F_6P{\cdot}C_4H_8O_2$	$C_{22}H_{20}AuBr_4N_4{\cdot}Br{\cdot}C_2H_3N$	$C_{24}H_{24}AuBr_4N_4{\cdot}Br$	$C_{32}H_{24}AuBr_4N_4{\cdot}Br$
Mr	443.91	410.95	461.98	1062.05	977.99	964.99	1061.07
Wave length [Å]	0.71073	1.54178	1.54178	0.71073	0.71073	0.71073	0.71073
Crystal system	Triclinic	Orthorhombic	Triclinic	Monoclinic	Triclinic	Monoclinic	Monoclinic
Space group	$P\bar{1}$	*Pnna*	$P\bar{1}$	*C2/c*	$P\bar{1}$	*C2/c*	$P2_1/n$
a [Å]	8.4901(2)	9.8442(5)	7.9523(5)	27.5547(5)	11.4138(5)	22.7764(4)	12.2854(3)
b [Å]	10.9180(3)	12.7548(3)	13.1938(11)	8.0827(1)	12.2346(5)	16.0601(2)	22.8693(3)
c [Å]	14.9044(4)	24.1456(8)	14.7836(12)	14.1653(3)	12.5493(5)	10.4146(2)	12.3872(3)
α [°]	98.417(2)		97.900(7)		65.243(4)		
β [°]	105.241(2)		99.511(6)	99.878(2)	68.992(4)	116.983(2)	114.445(3)
γ [°]	90.824(2)		104.142(7)		68.032(4)		
V [Å^3]	1316.59(6)	3031.7(2)	1457.6(2)	3108.07(10)	1432.81(12)	3394.86(11)	3168.31(14)
Z	4	8	4	4	2	4	4
ρ_{calc} [Mg m^{-3}]	2.240	1.801	2.105	2.270	2.267	1.888	2.224
μ [mm^{-1}]	8.47	9.70	8.71	9.99	12.13	10.24	10.98
Crystal size [mm^3]	0.29×0.21×0.08	0.21×0.14×0.11	0.44×0.11×0.03	0.35×0.18×0.12	0.33×0.22×0.10	0.19×0.13×0.11	0.22×0.18×0.04
2 θ_{max} [°]	65.3	134.5	134.5	58.5	74.8	64.6	65.6
Refls. collected	27,938	16,011	8840	24,060	51,397	35,134	39,864
Indep. reflections	8938	2708	8840	3973	14,450	5749	10,705
R_{int}	0.027	0.052	n/a (twin)	0.029	0.059	0.028	0.056
Max/min trans	0.548/0.184	1.0/0.717	1.0/0.877	0.403/0.152	0.368/0.087	1.0/0.686	0.677/0.189
Restrains/params	0/271	4/154	0/382	224/256	3/327	0/156	0/379
GooF on F^2	1.000	1.000	1.003	1.003	1.001	1.000	1.001
*R*1 [$I > 2\sigma(I)$]	0.0247	0.0479	0.0816	0.0184	0.0488	0.0249	0.0370
*wR*2 [$I > 2\sigma(I)$]	0.0596	0.1296	0.1952	0.0474	0.0807	0.0674	0.0685
*R*1(all data)	0.0339	0.0601	0.0917	0.0222	0.0942	0.0294	0.0626
*wR*2(all data)	0.0637	0.1395	0.2026	0.0491	0.1101	0.0699	0.0778
$\Delta\rho_{max/min}$ [e Å^{-3}]	1.12/−1.05	1.35/−1.25	3.73/−1.44	0.65/−0.61	4.03/−5.74	2.01/−2.23	1.25/−0.98
CCDC number	2074424	2074425	2074426	2074427	2074428	2074429	2074430

the each C_6 ring and the closest Br atom from the opposing molecule are 3.508 and 3.776 Å (Fig. 1b). The Br…C_6 (centroid) distances are shorter than the mean values (4.11 Å or 3.95 Å, depending on the details of the analysis) reported for C-Br…π interactions in the solid state structures of nucleic acids [31].

In the structure of the corresponding PF_6^- salt **8**, there are again two independent molecules, the 3,5-dibromophenyl moieties of the two molecules are "less parallel" than in **4** (Fig. 2a), but nevertheless they face one another and the distance between the centroids of the C_6 rings (3.948 Å) again suggests a π–π interaction (Fig. 2b).

The structure of 1-(3,5-dibromophenyl)-3-ethylimidazolium bromide **5** showed one independent molecule but with the ethylimidazolyl moiety disordered over two sites. In this structure the 3,5-dibromophenyl moieties in adjacent molecules are approximately perpendicular, with a Br atom from one molecule oriented toward the centroid of the C_6 ring of the next (Br…C_6 centroid ~ 3.547 Å) (Fig. 3b). In adjacent molecules the imidazolium moieties are approximately

Table 2 Selected bond distances (Å) and angles (°) for salts **4**, **5**, and **8** and complexes **10**–**13**

	C1-N2 C1-N5	N2-C1-N5 N2-C2-N5	Au1-C1	Au1-C2	C1-Au1-C2
4 Mol(1)	1.337(3) 1.32(3)	109(1)	–	–	–
Mol(2)	1.338(3) 1.32(1)	108.5(2)	–	–	–
5	1.340(9) 1.34(1)	108.0(7)	–	–	–
8 Mol(1)	1.35(1) 1.32(1)	109(1)	–	–	–
Mol(2)	1.35(2) 1.32(1)	109(1)	–	–	–
10	1.342(3) 1.359(3)	104.80(18)	2.023(2)	2.023(2)	180.00
11	1.346(6) 1.336(6)	104.6(4)	2.020(4)	2.025(4)	177.5(2)
12	1.359(3) 1.368(3)	103.7(2)	2.026(2)	2.026(2)	180.00(14)
13	1.355 5) 1.356(5)	104.6(3)	2.028(4)	2.028(4)	178.26(15)

parallel with a distance between the centroids of adjacent C_3N_5 rings being ~ 4.052 Å.

In the structure of **10**·EtOAc, the $[Au(NHC)_2]^+$ cation has inversion symmetry, and the two imidazolium moieties in the cation are coplanar (Fig. 4a). The two bromine atoms of each 3,5-dibromophenyl moiety in one cation have close contacts with the two imidazolyl moieties in an adjacent cation, so that the cations are arranged into chains (Fig. 4b).

In the structure of **11**·CH_3CN, the cation is no longer centrosymmetric. The NHC rings are inclined relative to one another by approximately 18.3° about the C-Au-C axis (approximating an anti arrangement around the Au centre, Fig. 5a). The cations are arranged in pairs. In these pairs, the intermolecular distance between imidazolyl ring centroids is 4.234 Å and the Au…Au distance is 4.476 Å, too large to be an aurophilic interaction. There are intermolecular Br…C_6 (centroid) contacts of 3.861 Å (Fig. 5b).

In the structure of **12**, the cation adopts a similar conformation to the cation in **10**·EtOAc, possessing an inversion centre and having its imidazolyl moieties coplanar (Fig. 6a). The cations are arranged into chains. The two Br atoms (Br53 and Br55) in each 3,5-dibromophenyl group are involved in different interactions. Br53 points toward an imidazolyl moiety in one adjacent cation and the Br55 atom in another adjacent cation. Br55 points toward the Br53 atom in one adjacent cation and the centroid of the 3,5-dibromophenyl C_6 ring in another adjacent cation (Fig. 6b). In the structure of **12**, the inter-cation Br53…C_3N_2 (centroid) distance is 4.689 Å, the Br55…C_6 (centroid) distance is 3.670 Å) and the Br53…Br55 distance is 3.606 Å, similar to the sum of the van der Waals radii, 3.66 Å as reported by Bondi [32].

In the structure of **13**, the cation adopts a conformation similar to the cation in **11**·CH_3CN with the two imidazolyl ring planes inclined ~ 8.68° with respect to each other. The cations form pairs. Within the pairs, the inter-cation distance between opposing imidazolyl rings is 3.717 Å, and the inter-cation Au…Au distance is 3.896 Å, too large to be considered an aurophilic interaction. There is an inter-cation π–π

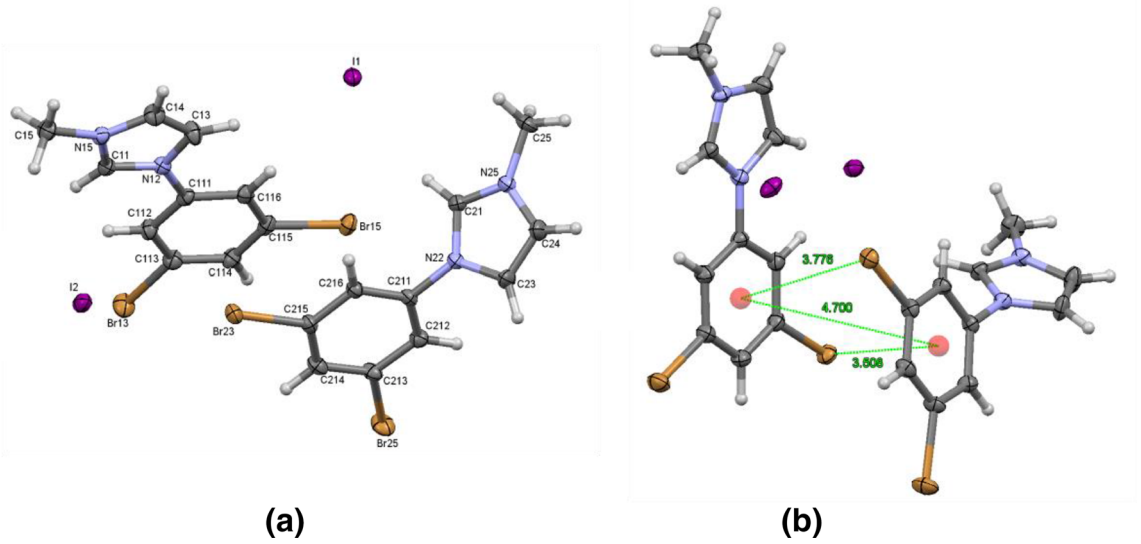

Fig. 1 Crystal structure of the **4** (50% level for the displacement ellipsoids). **a** The two independent molecules. **b** Interactions between the 3,5-dibromophenyl moieties of the two independent molecules

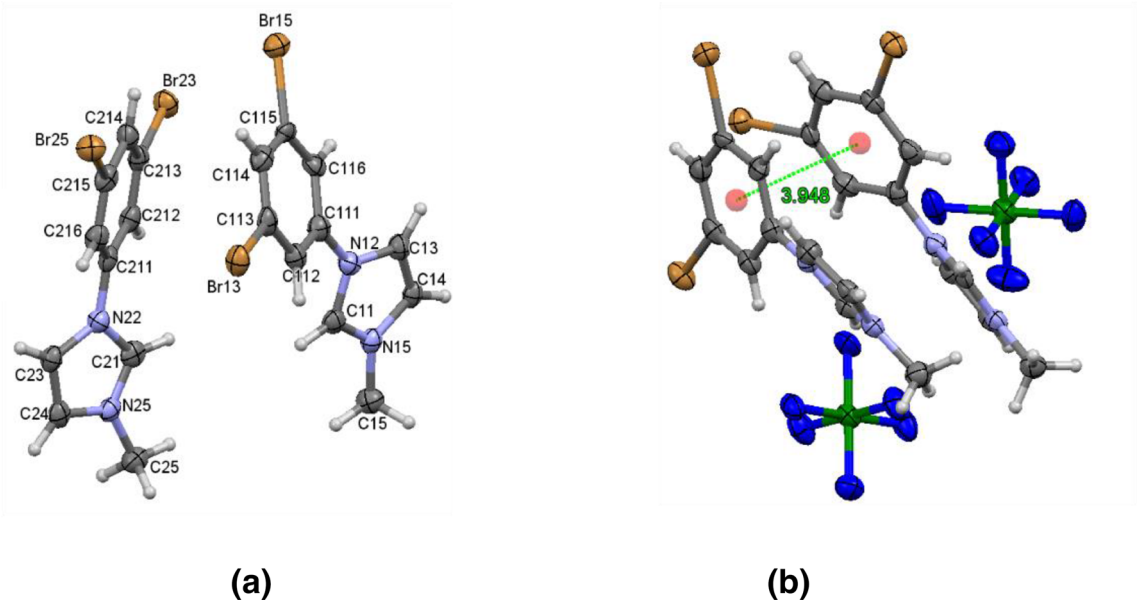

Fig. 2 Crystal structure of the **8** (50% level for the displacement ellipsoids). **a** The two independent cations. **b** The two independent cations and anions, showing the π–π interaction between the 3,5-dibromophenyl moieties

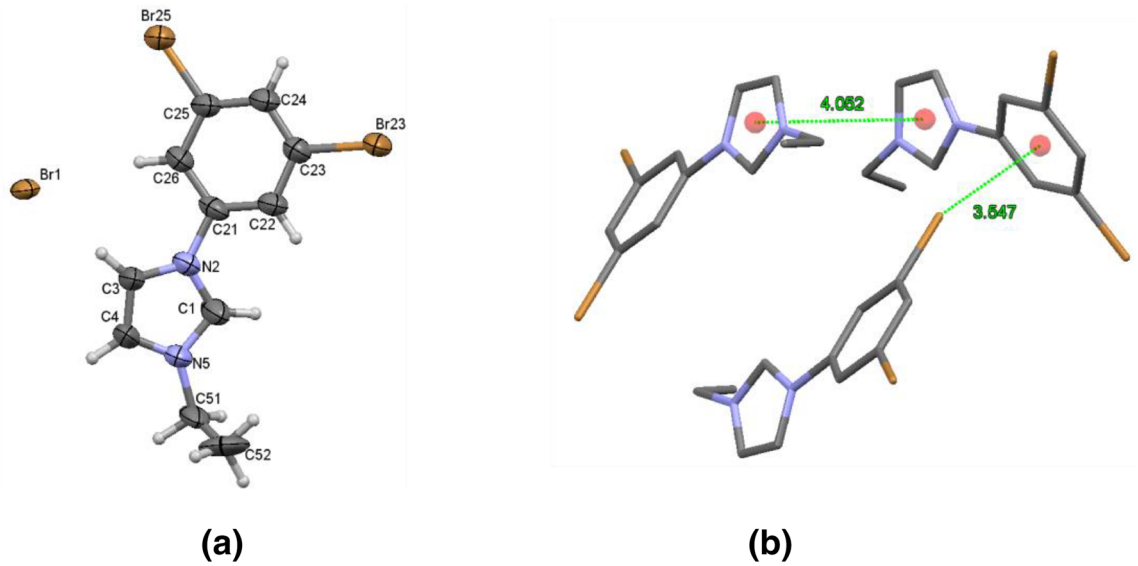

Fig. 3 Crystal structure of the **5**. **a** The major component of the cation (50% level for the displacement ellipsoids). **b** Three cations, showing Br-π interactions between 3,5-dibromophenyl moieties and π–π interactions between imidazolyl moieties (H atoms omitted for clarity)

interaction between 3,5-dibromophenyl moieties (distance between C_6 centroids = 3.817 Å) and an intra-cation Br…π interaction (Br…C_6 centroid distance = 4.063 Å) (Fig. 7b).

Activity of the Au-NHC complexes against OVCAR-8 cells

The new Au-NHC complexes containing one or more 3,5-dibromophenyl substituents on the NHC group showed notably high cytotoxic potency against OVCAR-8 cells (Table 3 and Fig. 8). The new Au-NHC complexes **9**–**13** were two orders of magnitude more cytotoxic than the

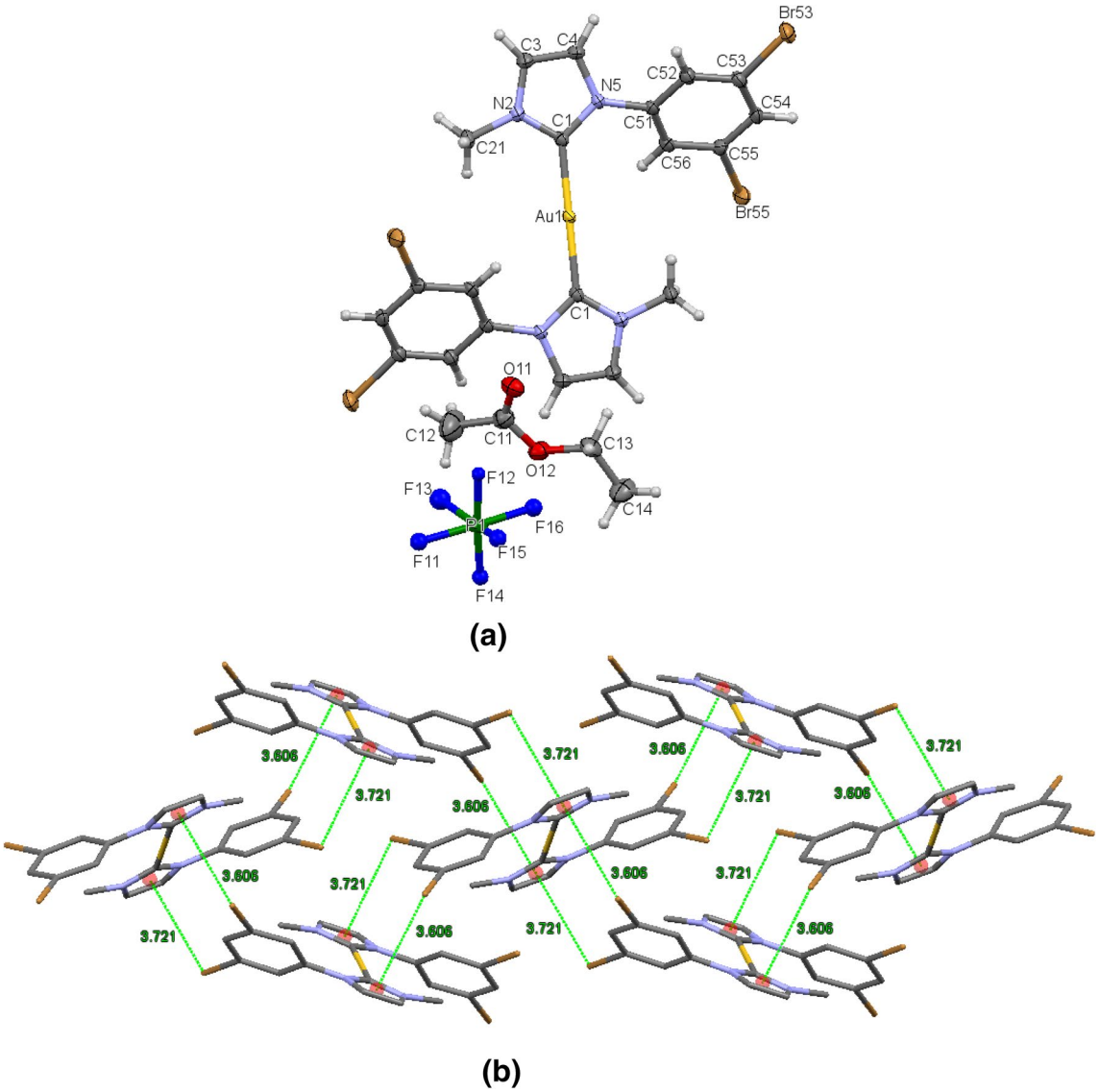

Fig. 4 Crystal structure of **10**·EtOAc. **a** The cation, anion, and associated EtOAc molecule (50% level for the displacement ellipsoids). **b** Chain of cations, showing close contact between Br in one cation and imidazolium moiety of the adjacent cation (H atoms omitted for clarity)

3,5-dibromophenyl-functionalised imidazolium salts **6** and **7**. All the complexes **9**–**13** are slightly more active than $[(Pr_2Im)_2Au]Br$ **14** (Pr_2Im = 1,3-dipropylimidazolin-2-ylidene; IC_{50} 1.0 ± 0.2, not shown in Fig. 8). This result is in accord with previous findings that lipophilicity is important in determining activity within the $[Au(NHC)_2]^+$ class [8, 14, 33, 34]. A recent study suggested introducing halogens into the NHC backbone can increase the activity of Au-NHCs in inhibition of TrxR isolated from rat liver, thus may affect the cytotoxicity of the compounds [34]. However, the *N*-phenyl-functionalised compound **9** showed very similar activity to its *N*-(3,5-dibromophenyl) analogue **12**, suggesting that the presence of bromine does not necessarily have a significant impact upon potency. Amongst the series of compounds **9–13**, the range of IC_{50} values is too small to indicate significant or obvious trends in activity with increasing lipophilicity.

It is important to mention that 1-(3,5-dibromophenyl)-3-isopropylimidazolium bromide **6** and 1-(3,5-dibromophenyl)-3-benzylimidazolium bromide **7** also have some inhibition activity at high concentration (IC_{50} ~ 47 μM and ~ 121 μM respectively), even though the diisopropylimidazolium bromide and diisopropylbenzimidazolium bromide were both found to be inactive (IC_{50} > 100 μM; results not shown in Fig. 8). It may be that the 3,5-dibromophenyl-functionalised imidazolium ions are sufficiently lipophilic to exert antimitochondrial activity as

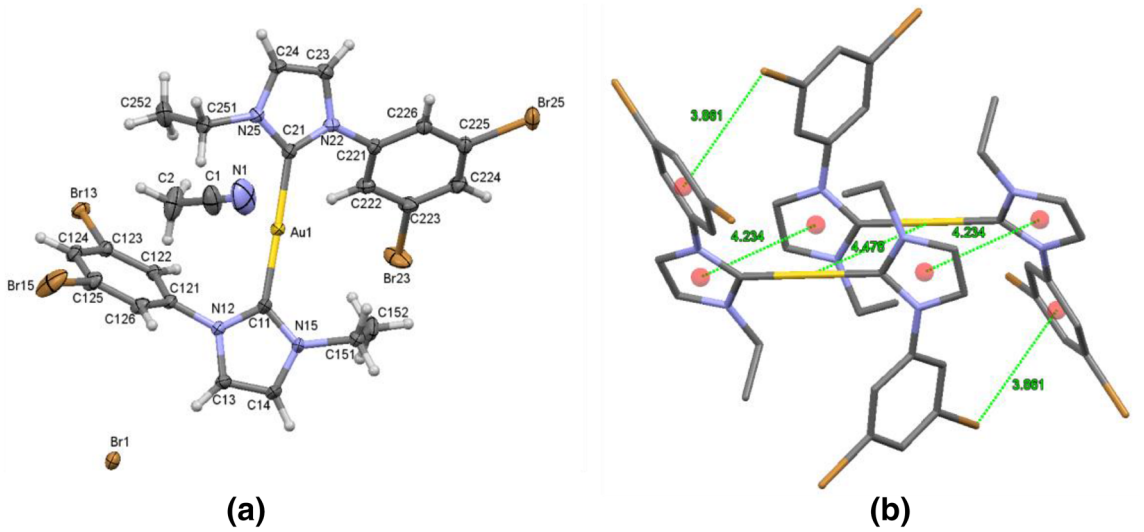

Fig. 5 Crystal structure of **11**·CH_3CN. **a** A cation, anion, and associated CH_3CN molecule (50% level for the displacement ellipsoids). **b** A pair of cations, showing inter-cation distances (H atoms omitted for clarity)

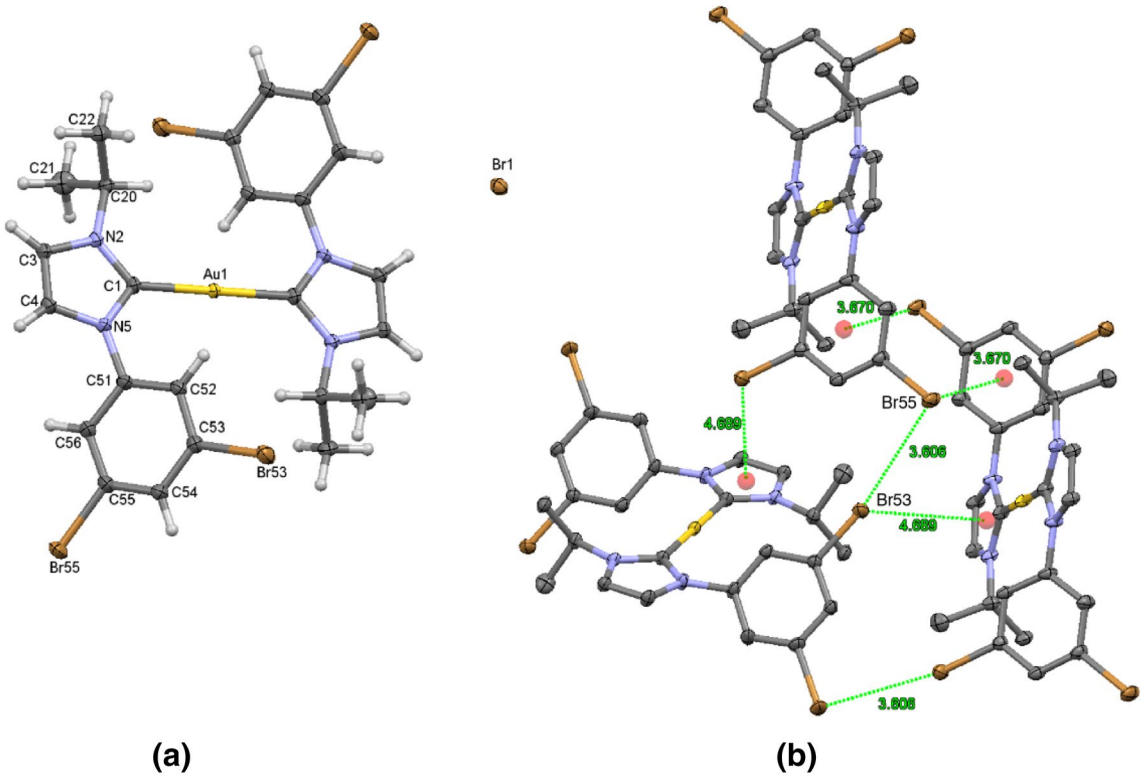

Fig. 6 Crystal structure of **12**. **a** A cation and associated anion (50% level for the displacement ellipsoids). **b** Three adjacent cations, showing inter-cation interactions (H atoms omitted for clarity)

delocalised lipophilic cations [4], whereas the other azolium ions are insufficiently lipophilic to exert activity.

It is interesting that within each of the pairs **12**, **13** and **6**, **7**, the presence of an isopropyl group instead of a benzyl group leads to higher activity against the OVCAR-8 cells. Intuitively, the compounds with the benzyl substituent should be more lipophilic than the compounds with the isopropyl substituent, but, nevertheless the presence of the

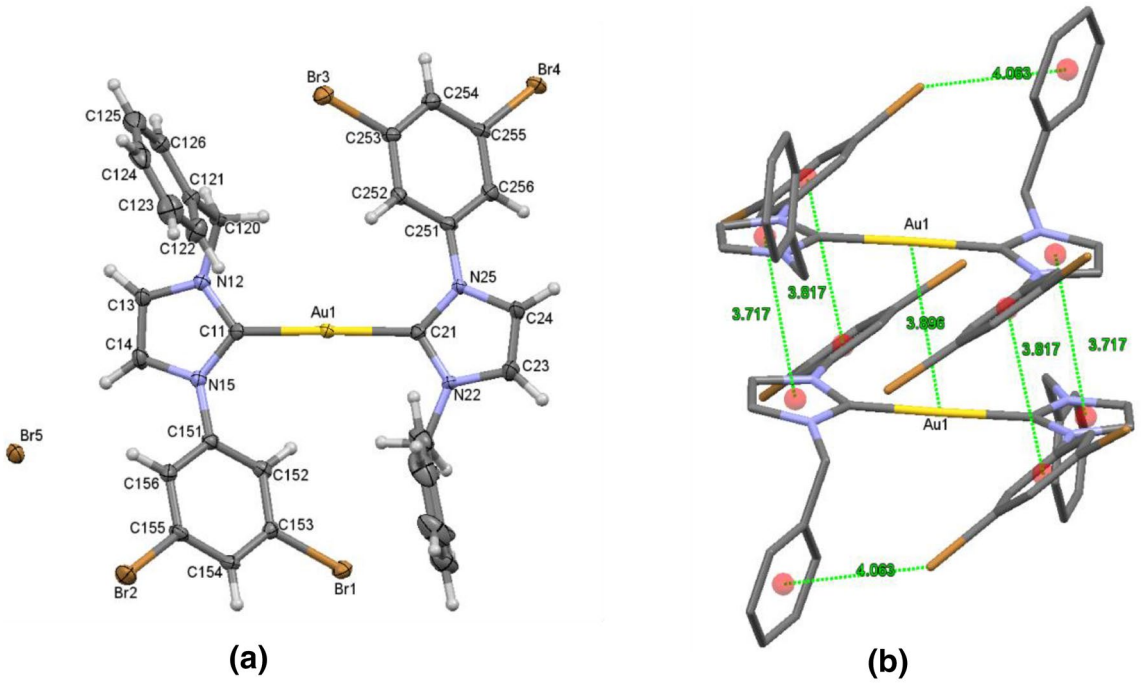

Fig. 7 Crystal structure of **13**. **a** A cation and associated anion (50% level for the displacement ellipsoids). **b** Two adjacent cations, showing inter-cation interactions (H atoms omitted for clarity)

Table 3 IC_{50} values for 3,5-dibromophenyl-functionalised Au-NHC complexes against OVCAR-8 cells

Compound	IC_{50} (μM) ± SEM	*n*
6[a]	47 ± 16	3
7[a]	121 ± 6	2
9	0.44 ± 0.04	3
10	0.63 ± 0.07	3
11	0.59 ± 0.06	3
12	0.322 ± 0.008	3
13	0.53 ± 0.08	3

OVCAR-8 cells were incubated with test compounds for 72 h and activity of the compounds on cell viability was evaluated using an MTT assay. Data are shown as mean ± SEM of three independent experiments (*n*) each of which used 2–4 replicates per concentration for a test compound

[a]Imidazolium salts **6** and **7** used as a negative control

isopropyl group instead of the benzyl group appears to be advantageous. In the solid state (Figs. 6 and 7), the isopropyl-functionalised cation in **12** adopts a more planar conformation than its benzyl-functionalised counterpart in **13**, but whether the conformation of the cations is responsible for the difference in activities of **12** and **13** requires further investigation. We note that in the ^{1}H NMR spectrum of **13**, the number of signals and their splitting patterns indicate there is only a single benzyl environment. This result in turn indicates that there must be some rotation of the NHC ligands about the Au-C axis on the NMR timescale, so that the structure seen in the solid state does not remain rigid in solution, so the relevance of the solid state structures of **12** and **13** to the biological results is unclear.

Experimental

Nuclear magnetic resonance spectra were recorded using Bruker Bruker ARX500 (500.13 MHz for ^{1}H, 125.77 MHz for ^{13}C and 202.45 MHz for ^{31}P), or Bruker ARX600 (600.13 MHz for ^{1}H, 150.90 MHz for ^{13}C) spectrometers at ambient temperature unless otherwise indicated. ^{1}H and ^{13}C NMR chemical shifts were referenced to the residual signal of the solvent (DMSO-d_6: ^{1}H 2.50 ppm; ^{13}C 39.52 ppm. and ^{31}P chemical shifts were referenced to an external 85% H_3PO_4 solution. ^{1}H-^{13}C HSQC (heteronuclear single quantum coherence), ^{1}H-^{13}C HMBC (heteronuclear multiple bond correlation) were used to assign signals, and microanalysis were performed by The School of Chemistry & Molecular Biosciences, University of Queensland, Australia. High resolution mass spectra were measured using *Agilent* LCMS 6510 Q-TOF or Waters LCT Premier XE spectrometers, using the ESI method, with CH_3CN:H_2O (9:1) as solvent. All organometallic compounds were prepared under a nitrogen atmosphere and in dark by using aluminium foil. Chromatography was performed on silica (Davisil) unless otherwise stated. Crystallographic data were measured at 100(2) K on either an Oxford Diffraction Gemini or an

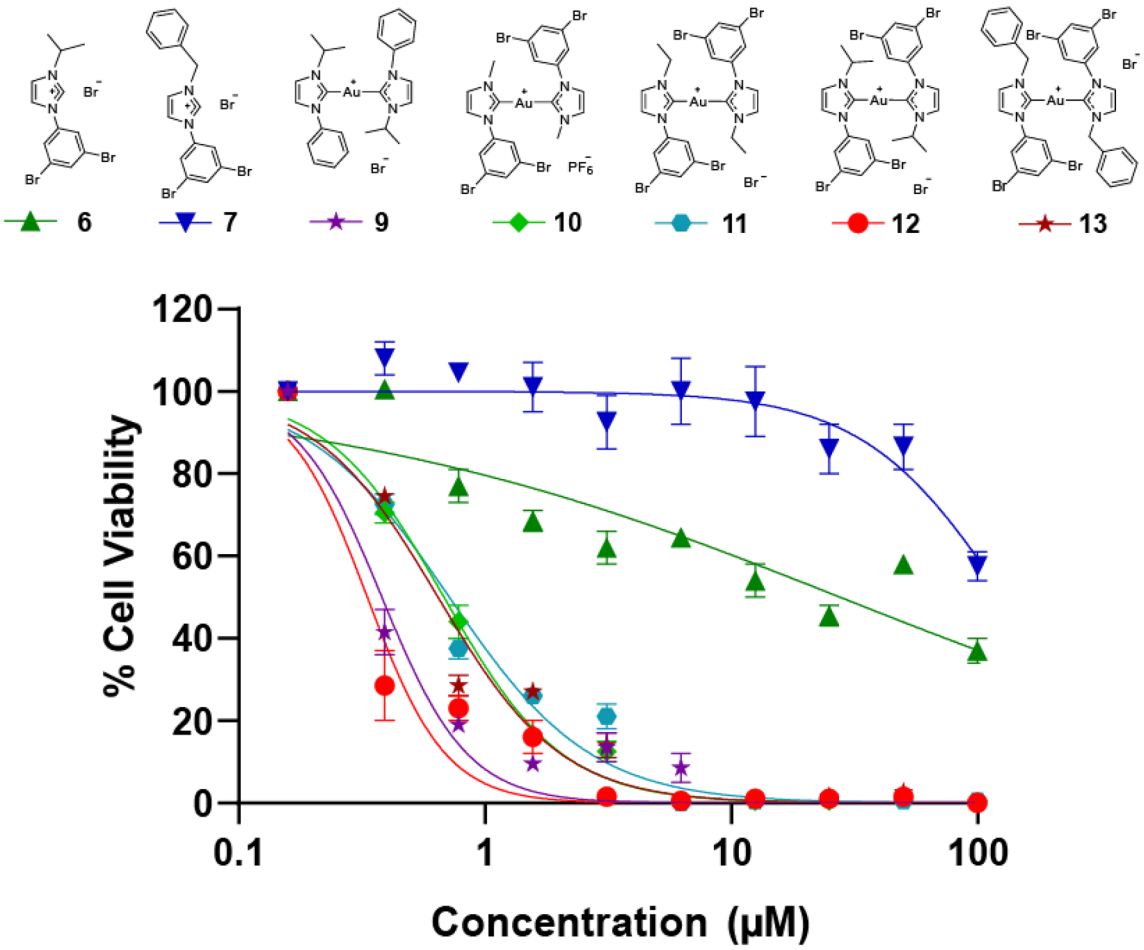

Fig. 8 The inhibition activity of the 3,5-dibromophenyl-functionalised Au-NHC complexes **9–13** against OVCAR-8 cells, measured by MTT assay after 72 h of treatment. The imidazolium salts **6** and **7** were used as negative controls. Data are shown as mean ± SEM of $n = 3$ independent experiments, each of which used 2 to 4 replicates per concentration for a test compound

Oxford Diffraction Xcalibur diffractometer using Mo Kα or Cu Kα radiation. Following analytical absorption corrections and solution by direct methods, the structures were refined against F^2 with full-matrix least-squares using the SHELX program suite [35]. Unless stated differently below, all hydrogen atoms were added at calculated positions and refined by use of riding models. Except for those atoms mentioned below, anisotropic displacement parameters were employed throughout for the non-hydrogen atoms. Residual electron density in the crystal of compounds **5** and **12**, which could not be interpreted as chemically reasonable moieties, was effectively removed by use of the program SQUEEZE [36]. Crystallographic data for the structures reported in this paper have been deposited at the Cambridge Crystallographic Data Centre. Copies of data with CCDC numbers 2074424-2074430 can be obtained free of charge via https://www.ccdc.cam.ac.uk/structures/, or from the Cambridge Crystallographic Data Centre, 12 Union Road, Cambridge CB2 1EZ, UK (fax +441223336033; email deposit@ccdc.cam.ac.uk).

Materials

The following compounds were used as received: potassium carbonate (Analar Normapur), potassium hexafluorophosphate (Aldrich, 98%), imidazole (Fluka), 1,3,5-tribromobenzene (BDH), bromobenzene (Fluka), sodium hydroxide (Chem Supply), magnesium sulfate anhydrous (Scharlau), 2-bromopropane (Acros Organics), bromoethane (Ajax), methyl iodide, benzyl bromide (Merck). The solvents were of analytical grade and used without further drying.

Synthesis of 1-phenylimidazole (1)

Sodium hydroxide (950 mg, 23.7 mmol) was added to a solution of imidazole (1.50 g, 22.0 mmol) in DMSO (10 mL)

and the mixture was stirred for 30 min at room temperature. Bromobenzene (2.3 mL, 22.0 mmol) was added, followed by cuprous oxide (180 mg, 1.26 mmol). The mixture was heated at 100 °C overnight. The mixture was diluted with H_2O (100 mL) and extracted with dichloromethane (8 × 25 mL). The combined organic layer was evaporated under reduced pressure. The green residue was suspended in H_2O (50 mL), the mixture was filtered, and the green solid that was collected was washed with H_2O (3 × 10 mL) and dried, then dissolved in dichloromethane (200 mL). The clear green solution was dried over $MgSO_4$ and evaporated. The resulting green oily residue was purified by flash column chromatography eluting with 3:2 ethyl acetate/cyclohexane. The product was obtained as a yellow oil (1.70 g, 53%). ^{1}H NMR (500 MHz, DMSO-d_6): δ 8.25 (1H, apparent t, splitting 1.1 Hz, imidazolyl H2), 7.74 (1H, apparent t, splitting 1.2 Hz, imidazolyl H4 or H5), 7.63–7.66 (2H, m, ArH *ortho*), 7.53–7.49 (2H, m, ArH *meta*), 7.36 (1H, m, ArH *para*), 7.10 (1H, apparent t, splitting 1.2 Hz, imidazolyl H5 or H4). NMR data are consistent with literature values [37].

Synthesis of 3,5-dibromophenylimidazole (2)

Sodium hydroxide (480 mg, 12.0 mmol) was added to a solution of imidazole (681 mg, 10.0 mmol) in DMSO (20 mL) and the mixture was stirred for 60 min at room temperature. 1,3,5-Tribromobenzene (3.50 g, 11.1 mmol) was added followed by cuprous oxide (90.0 mg, 0.63 mmol). The mixture was heated at 100 °C for 48 h. The mixture was diluted with H_2O (200 mL) and a dark grey precipitate formed, which was filtered off and washed with H_2O several times. The solid dried then suspended in dichloromethane (250 mL) and stirred at room temperature, then the dark brown solution was filtered through a plug of Celite, and the orange filtrate was evaporated to dryness. The orange residue was purified by flash column chromatography eluting with 2:1 ethyl acetate/cyclohexane. The product was obtained as a pale yellow solid (1.27 g, 42%). ^{1}H NMR (500 MHz, $CDCl_3$): δ 7.84 (br apparent t, splitting 1.2 Hz, 1H, imidazolyl H2), 7.67 (1H, t, $^4J_{H,H}$ = 1.6 Hz, ArH *para*), 7.51 (2H, d, $^4J_{H,H}$ = 1.6 Hz, ArH *ortho*), 7.25 (1H, apparent t, splitting 1.3 Hz, imidazolyl H4 or H5), 7.22 (1H, br apparent t, splitting 1.3 Hz, imidazolyl H5 or H4). NMR data are consistent with literature values [37].

Synthesis of 1-phenyl-3-isopropylimidazolium bromide (3)

A mixture of 1-phenylimidazole (0.22 mL, 1.73 mmol) and isopropyl bromide (26.2 mL, 279 mmol) were dissolved in ethyl acetate (20 mL). The solution was refluxed for 12 days. The mixture was cooled to room temperature and the solvent and isopropyl bromide evaporated under reduced pressure. The oily residue was triturated with diethyl ether (20 mL), the diethyl ether was decanted off, and the trituration was repeated twice more. Traces of ether were removed under flow of N_2, and the oily residue was purified by column chromatography, eluting with a mixture of dichloromethane (100 mL) and acetonitrile (15 mL). The colourless product was triturated with diethyl ether (3 × 20 mL), and removal of residual ether under a flow N_2 left 1-phenyl-3-isopropylimidazolium bromide as a colourless hygroscopic solid (320 mg, 69%). ^{1}H NMR (500 MHz, DMSO-d_6): δ 9.90 (1H, apparent t, splitting 1.5 Hz, imidazolyl H2), 8.38 (1H, apparent t, splitting 1.7 Hz, imidazolyl H4), 8.20 (1H, apparent t, splitting 1.7 Hz, m, imidazolyl H5), 7.8 (2H, m, ArH *ortho*), 7.67 (2H, m, ArH *meta*), 7.60 (1H, m, ArH *para*), 4.74 (1H, sept, $^3J_{H,H}$ = 6.7 Hz, C*H*(CH_3)$_2$), 1.57 (6H, d, $^3J_{H,H}$ = 6.7 Hz, CH(C*H*$_3$)$_2$). ^{13}C NMR (125.7 MHz, DMSO-d_6): δ 134.85 (ArC *ipso*), 134.21 (imidazolyl C2) 130.11 (ArC *meta*), 129.68 (ArC *para*), 121.88 (ArC *ortho*), 121.53 (imidazolyl C5), 121.23 (imidazolyl C4), 52.94 (*C*H(CH_3)$_2$); 22.24 (CH(*C*H$_3$)$_2$). Microanalysis: Found: C, 52.19; H, 5.84; N, 10.14% $C_{12}H_{15}BrN_2.(H_2O)_{0.5}$ requires. C, 52.08; H, 5.73; N, 10.06%.

Synthesis of 1-(3,5-Dibromophenyl)-3-methyllimidazolium iodide (4)

Methyl iodide (0.52 mL, 8.41 mmol) was added to a solution of 1-(3,5-dibromophenyl)imidazole (1.00 g, 3.31 mmol) in ethyl acetate (40 mL). The mixture was refluxed overnight. The solvent was evaporated by flow of N_2, and the product was stirred with diethyl ether (3 × 50 mL), then was filtered off and dried in air to leave a beige powder (505 mg, 35%). ^{1}H NMR (500 MHz, DMSO-d_6): δ 9.84 (br s, 1H, imidazolyl H2), 8.34 (1H, apparent t, splitting 1.7 Hz, imidazolyl H5), 8.14 (2H, d, $^4J_{H,H}$ = 1.7 Hz, ArH *ortho*), 8.11 (1H, t, $^4J_{H,H}$ = 1.7 Hz, ArH *para*), 7.94 (1H, br apparent t, splitting 1.6 Hz, imidazolyl H4), 3.93 (s, 3H, CH_3).^{13}C NMR (125.7 MHz, DMSO-d_6): δ 136.70 (imidazolyl C2), 134.54 (ArC *para*), 124.38 (imidazolyl C4), 124.03 (ArC *ortho*), 123.43 (ArC-Br), 121.00 (imidazolyl C5); 36.27 (CH_3). Microanalysis: Found: C, 27.38; H, 2.05; N, 6.06% $C_{10}H_9Br_2IN_2$ requires C, 27.06; H, 2.04; N, 6.31%. Crystals suitable for X-ray diffraction studies were grown by diffusion of vapours between diethyl ether and a solution of the imidazolium salt (**4**) in acetonitrile.

Synthesis of 1-(3,5-Dibromophenyl)-3-ethyllimidazolium bromide (5)

1-(3,5-Dibromophenyl)imidazole (350 mg, 1.16 mmol) and ethyl bromide (10.0 mL, 134 mmol) were combined and the mixture was refluxed for 7 days. The mixture was cooled to room temperature and the product was filtered

off and washed with diethyl ether (3 × 30 mL) and dried under flow of N_2 to leave the product as a white solid (320 mg, 67%). ^{1}H NMR (600 MHz, DMSO-d_6): δ 9.88 (1H, apparent t, splitting 1.6 Hz, imidazolyl H2), 8.37 (1H, apparent t, splitting 1.8 Hz, imidazolyl H5), 8.18 (2H, d, $^4J_{H,H}$ = 1.6 Hz, ArH *ortho*), 8.11 (1H, t, $^4J_{H,H}$ = 1.6 Hz, ArH *para*), 8.05 (1H, apparent t, splitting 1.8 Hz, imidazolyl H4), 4.27 (2H, q, $^3J_{H,H}$ = 7.3 Hz, C*H*$_2$CH$_3$), 1.50 (3H, t, $^3J_{H,H}$ = 7.3 Hz, CH$_2$C*H*$_3$). ^{13}C NMR (150.90 MHz, DMSO-d_6): δ 136.75 (ArC *ipso*), 135.84 (imidazolyl C2) 134.48 (ArC *para*), 124.00 (ArC *ortho*), 123.39 (ArC-Br), 123.03 (imidazolyl C4), 121.06 (imidazolyl C5), 44.94 (*C*H$_2$CH$_3$); 14.66 (CH$_2$*C*H$_3$). Microanalysis: Found: C, 32.48; H, 2.88; N, 6.44% $C_{11}H_{11}Br_2N_2$ requires C, 32.15; H, 2.70; N, 6.82%. HRMS (ESI$^+$): Calcd for $C_{11}H_{11}Br_2N_2$ [M-Br$^+$], 328.9289 m/z. Found, *m/*z 328.9305. Crystals suitable for X-ray diffraction studies were grown by diffusion of vapours between diethyl ether and a solution of the imidazolium salt (**5**) in methanol.

Synthesis of 1-(3,5-dibromophenyl)-3-isopropylimidazolium bromide (6)

1-(3,5-Dibromophenyl)imidazole (670 mg, 2.22 mmol) and isopropyl bromide (22 mL, 234 mmol) were combined and the mixture was refluxed for 14 days. The mixture was cooled to room temperature and the product was filtered off and washed with diethyl ether (3 × 30 mL) and dried under a flow of N_2 to leave the product as a beige solid (700 mg, 74%). ^{1}H NMR (500 MHz, DMSO-d_6): δ 9.88 (1H, apparent t, splitting 1.6 Hz, imidazolyl H2), 8.39 (1H, apparent t, splitting 1.9 Hz, imidazolyl H5), 8.20 (2H, d, $^4J_{H,H}$ = 1.6 Hz, ArH *ortho*), 8.15 (1H, apparent t, splitting 1.9 Hz, imidazolyl H4), 8.10 (1H, t, $^4J_{H,H}$ = 1.6 Hz, ArH *para*), 4.68 (1H, sept., $^3J_{H,H}$ = 6.6 Hz, (C*H*(CH$_3$)$_2$), 1.55 (6H, d, $^3J_{H,H}$ = 6.6 Hz, CH(C*H*$_3$)$_2$).^{13}C NMR (125.7 MHz, DMSO-d_6): δ 136.81 (ArC *ipso*), 135.89 (imidazolyl C2) 134.45 (ArC *para*), 124.04 (ArC *ortho*), 123.37 (ArC-Br), 121.68 (imidazolyl C4), 121.18 (imidazolyl C5), 53.20 (*C*H(CH$_3$)$_2$); 22.16 (CH(*C*H$_3$)$_2$).Microanalysis: Found: C, 33.32; H, 3.00; N, 6.37% $C_{12}H_{13}Br_3N_2$ $(H_2O)_{0.2}$ requires. C, 33.63; H, 3.15; N, 6.54%. HRMS (ESI$^+$): Calcd for $C_{12}H_{13}Br_2N_2$ [M-Br$^+$], *m/*z 342.9445. Found, *m/*z 342.9426.

Synthesis of 1-(3,5-dibromophenyl)-3-benzylimidazolium bromide (7)

1-(3,5-Dibromophenyl)imidazole (500 mg, 1.65 mmol) and benzyl bromide (0.40 mL, 3.36 mmol) were dissolved in toluene (30 mL) and the clear solution was refluxed for 2 days. The mixture was cooled to room temperature and the product was filtered off and washed with diethyl ether (3 × 20 mL) and dried under vacuum to leave the product as a white powder (650 mg, 83%). ^{1}H NMR (600 MHz, DMSO-d_6): δ 10.0 (1H, apparent t, splitting 1.6 Hz, imidazolyl H2), 8.40 (1H, apparent t, splitting 1.8 Hz, imidazolyl H5), 8.20 (2H, d, $^4J_{H,H}$ = 1.6 Hz, $C_6H_3Br_2$ H *ortho*), 8.12 (1H, t, $^4J_{H,H}$ = 1.6 Hz, $C_6H_3Br_2$ H *para*), 8.03 (1H, apparent t, splitting 1.8 Hz, imidazolyl H4), 7.51–7.41 (5H, m, Ph-H), 5.50 (s, 2H, CH$_2$). ^{13}C NMR (150.90 MHz, DMSO-d_6): δ 136.7 ($C_6H_3Br_2$ C *ipso*), 136.3 (imidazolyl C2) 134.5 (Ph C *ipso*), 134.2 ($C_6H_3Br_2$ C *para*), 129.0 (Ph C *meta*), 128.8 (Ph C *para*), 128.5 (Ph C *ortho*), 124.2 ($C_6H_3Br_2$ C *ortho*), 123.3 ($C_6H_3Br_2$ C-Br); 123.1 (imidazolyl C4); 121.7 (imidazolyl C5), 52.54 (CH$_2$). Microanalysis: Found: C, 40.93; H, 2.58; N, 5.68% $C_{16}H_{13}Br_3N_2$. requires. C, 40.63; H, 2.77; N, 5.92%. HRMS (ESI$^+$): Calcd for $C_{16}H_{13}Br_2N_2$ [M-Br$^+$], *m/*z 390.9445. Found, *m/*z 390.9432.

Synthesis of 1-(3,5-dibromophenyl)-3-methyllimidazolium hexafluorophosphate (8)

Potassium hexafluorophosphate (230 mg, 1.26 mmol) in (5 mL) H_2O was added to a solution of 1-(3,5-dibromophenyl)-3-methylimidazolium iodide (224 mg, 0.503 mmol) in 1:1 H_2O:MeOH (4 mL each), and a white precipitate formed immediately. The mixture was stirred at room temperature overnight. The precipitate was filtered off, washed with H_2O (2 × 10 mL) and dried under vacuum to leave a white powder (178 mg, 77%). ^{1}H NMR (500 MHz, DMSO-d_6): δ 9.82 (1H, br s, imidazolyl H2), 8.34 (1H, apparent t, splitting 1.8 Hz, imidazolyl H5), 8.14 (2H, d, $^4J_{H,H}$ = 1.7 Hz, ArH *ortho*), 8.11 (1H, t, $^4J_{H,H}$ = 1.7 Hz, ArH *para*), 7.93 (1H, apparent t, splitting 1.8 Hz, imidazolyl H4), 3.92 (s, 3H, CH$_3$). ^{31}P NMR (202.45 MHz, DMSO-d_6): δ -144.2 (sept., $^1J_{P,F}$ = 708 Hz, 1P, PF_6^-). Microanalysis: Found: C, 26.18; H, 2.04; N, 5.80% $C_{10}H_9Br_2F_6N_2P$ requires C, 26.00; H, 1.96; N, 6.06%. Crystals suitable for X-ray diffraction studies were grown by diffusion of vapours between diethyl ether and a solution of the imidazolium salt (**8**) in acetonitrile.

Bis(1-phenyl-3-isopropylimidazolin-2-ylidene) gold(I) bromide (9)

1-Phenyl-3-isopropylimidazolium bromide (72.7 mg, 0.27 mmol) and potassium carbonate (380 mg, 2.72 mmol) were stirred in acetonitrile (10 mL) at room temperature for 5 min. (Me$_2$S)AuBr (44.6 mg, 0.131 mmol) was added and the mixture was stirred for 24 h. The mixture was filtered through Celite and the filtrate evaporated to dryness, to leave the product as an off-white powder (71 mg, 82%). ^{1}H NMR (500 MHz, DMSO-d_6): δ 7.91–7.90 (4H, m, imidazolyl H5 and imidazolyl H4), 7.73–7.71 (4H, m, ArH *ortho*), 7.55–7.54 (6H, m, ArH *meta* and ArH *para*), 4.70 (2H, sept, $^3J_{H,H}$ = 6.7 Hz, C*H*(CH$_3$)$_2$), 1.42 (12H, d, $^3J_{H,H}$ = 6.7 Hz,

$CH(CH_3)_2$) ^{13}C NMR (125.7 MHz, DMSO-d_6): δ 180.06 (C2), 139.02 (ArC *ipso*) 129.50 (ArC *meta*), 128.96 (ArC *para*), 124.94 (C *ortho*), 123.22 (C5), 119.60 (C4), 53.52 $CH(CH_3)_2$; 22.85 $CH(CH_3)_2$. Microanalysis: Found: C, 38.80; H, 4.86; N, 7.11% $C_{24}H_{28}AuBrN_4.(H_2O)_5$ requires C, 38.98; H, 5.18; N, 7.58%.

Bis(1-(3,5-dibromophenyl)-3-methylimidazolin-2-ylidene)gold(I) hexafluorophosphate (10)

1-(3,5-Dibromophenyl)-3-methylimidazolium hexafluorophosphate (50.0 mg, 0.108 mmol) and potassium carbonate (200 mg, 1.44 mmol) were stirred in acetonitrile (5 mL) at room temperature for 5 min. $(Me_2S)AuCl$ (16.0 mg, 0.054 mmol) was added and the mixture was stirred for 24 h. The mixture was filtered through Celite and the filtrate was evaporated to dryness. The residue was recrystallised from ethyl acetate to leave the product as light yellow crystals (30 mg, 57%). ^1H NMR (500 MHz, DMSO-d_6): δ 8.03 (4H, d, $^4J_{H,H}$ = 1.7 Hz, ArH *ortho*), 7.97 (2H, t, $^4J_{H,H}$ = 1.7 Hz, ArH *para*), 7.96 (2H, d, $^3J_{H,H}$ = 1.8 Hz, imidazolyl H5), 7.74 (2H, d, $^3J_{H,H}$ = 1.8 Hz, imidazolyl H4), 3.90 (s, 6H, CH_3). ^{13}C NMR (125.7 MHz, DMSO-d_6): δ 181.68 (imidazolyl C2), 140.63 (ArC *ipso*), 133.97 (ArC *para*), 126.87 (ArC *ortho*), 124.48 (imidazolyl C4), 122.88 (imidazolyl C5), 122.76 (ArC-Br); 37.94 (CH_3). Microanalysis: Found: C, 26.97; H, 2.09; N 5.19% $C_{20}H_{16}AuBr_4F_6N_4P$. $(CH_3CH_2OCOCH_3)_{0.8}$ requires C, 26.68; H, 2.16; N, 5.36%. HRMS (ESI^+): Calcd for $C_{20}H_{16}Br_4N_4Au$ [M-PF_6^+], m/z 824.7775. Found, *m/z* 824.7774. Crystals suitable for X-ray diffraction studies were grown by recrystallisation from ethyl acetate.

Bis(1-(3,5-dibromophenyl)-3-ethylimidazolin-2-ylidene)gold(I) bromide (11)

1-(3,5-Dibromophenyl)-3-ethylimidazolium bromide (83.7 mg, 0.20 mmol) and potassium carbonate (270 mg, 1.95 mmol) were stirred in acetonitrile (5 mL) at room temperature for 5 min. $(Me_2S)AuBr$ (29.1 mg, 0.086 mmol) was added and the mixture was stirred for 24 h. The mixture was filtered through Celite and the filtrate removed to dryness. The residue was recrystallised from acetonitrile/diethyl ether and dried under vacuum to leave the product as a beige powder (69 mg, 86%). ^{1}HNMR (500 MHz, DMSO-d_6): δ 8.03 (4H, d,$^4J_{H,H}$ = 1.7 Hz, ArH *ortho*), 8.01 (2H, t,$^4J_{H,H}$ = 1.7 Hz, ArH *para*), 7.94 (2H, d, $^3J_{H,H}$ = 1.9 Hz, imidazolyl H5), 7.84 (2H, d, $^3J_{H,H}$ = 1.9 Hz, imidazolyl H4), 4.22 (4H, q, $^3J_{H,H}$ = 7.3 Hz, $CH_2(CH_3)_2$), 1.4 (6H, t, $^3J_{H,H}$ = 7.3 Hz, $CH_2(CH_3)_2$). ^{13}C NMR (125.7 MHz, DMSO-d_6): δ 181.4 (imidazolyl C2), 141.3 (ArC *ipso*), 134.5 (ArC *para*), 127.6 (ArC *ortho*), 123.6 (imidazolyl C5), 123.3 (ArC-Br), 123.2 (imidazolyl C4), 46.6 $CH_2(CH_3)_2$, 16.9 $CH_2(CH_3)_2$. Microanalysis: Found: C, 28.31; H, 2.28; N, 5.76% $C_{22}H_{20}AuBr_5N_4$. $(H_2O)_{0.2}$ requires C, 28.09; H, 2.19; N, 5.96%. HRMS (ESI^+): Calcd for $C_{22}H_{20}Br_4N_4Au$ [M-Br^+], m/z 852.8087. Found, *m/z* 852.8118. Crystals suitable for X-ray diffraction studies were grown by diffusion of vapours between diethyl ether and a solution of complex **11** in acetonitrile.

Bis(1-(3,5-dibromophenyl)-3-isopropylimidazolin-2-ylidene)gold(I) bromide (12)

1-(3,5-Dibromophenyl)-3-isopropylimidazolium bromide (100 mg, 0.235 mmol) and potassium carbonate (330 mg, 2.38 mmol) were stirred in acetonitrile (5 mL) at room temperature for 5 min. $(Me_2S)AuBr$ (40.0 mg, 0.117 mmol) was added and the mixture was stirred for 24 h. The mixture was filtered through Celite and the filtrate evaporated to dryness. The residue was recrystallised from acetonitrile/diethyl ether and dried under vacuum to leave the product as an off-white powder (85 mg, 75%). ^1H NMR (500 MHz, DMSO-d_6): δ 8.05 (2H, t, $^4J_{H,H}$ = 1.6 Hz, ArH *para*), 8.04 (4H, d, $^4J_{H,H}$ = 1.6 Hz, ArH *ortho*), 7.94 (2H, d, $^3J_{H,H}$ = 1.9 Hz, imidazolyl H5), 7.92 (2H, d, $^3J_{H,H}$ = 1.9 Hz, imidazolyl H4), 4.67 (2H, sept, $^3J_{H,H}$ = 6.7 Hz, $CH(CH_3)_2$), 1.44 (12H, d, $^3J_{H,H}$ = 6.7 Hz, $CH(CH_3)_2$). ^{13}C NMR (125.7 MHz, DMSO-d_6): δ 180.29 (C2), 141.11 (ArC *ipso*) 134.15 (ArC *para*), 127.56 (ArC *ortho*), 123.59 (imidazolyl C5), 122.83 (ArC-Br), 119.79 (imidazolyl C4), 53.84 $CH(CH_3)_2$)); 22.93 $CH(CH_3)_2$). Microanalysis: Found: C, 29.50 H, 2.31; N, 5.53% $C_{24}H_{24}AuBr_5N_4$ requires C, 29.87; H, 2.51; N, 5.81%. HRMS (ESI^+): Calcd for $C_{24}H_{24}Br_4N_4Au$ [M-Br^+], m/z 880.8400. Found, *m/z* 880.8420. Crystals suitable for X-ray diffraction studies were grown by diffusion of vapours between pentane and a solution of complex **12** in dichloromethane.

Bis(1-(3,5-dibromophenyl)-3-benzylimidazolin-2-ylidene)gold(I) bromide (13)

1-(3,5-Dibromophenyl)-3-benzylimidazolium bromide (100 mg, 0.21 mmol) and potassium carbonate (290 mg, 2.09 mmol) were stirred in acetonitrile/ethanol (4:1 mL) at room temperature for 5 min. $(Me_2S)AuBr$ (31.0 mg, 0.091 mmol) was added and the mixture was stirred for 24 h. The mixture was filtered through Celite and the filtrate evaporated to dryness. The residue was recrystalised from acetonitrile/diethyl ether and dried under vacuum to leave the product as a white powder (89 mg, 92%). ^1H NMR (500 MHz, DMSO-d_6): 8.04 (4H, d, $^4J_{H,H}$ = 1.7 Hz, ArH *ortho*), 7.97 (2H, d, $^3J_{H,H}$ = 1.9 Hz, imidazolyl H5), 7.89 (2H, t, $^4J_{H,H}$ = 1.7 Hz, ArH *para*), 7.85 (2H, m, imidazolyl H4), 7.31–7.27 (6H, m, Ph-H *meta* and Ph-H *para*), 7.19 (4H, m, Ph-H *ortho*), 5.37 (s, 4H, CH_2). ^{13}C NMR (125.7 MHz,

DMSO-d_6): δ 181.4 (imidazolyl C2), 140.7 ($C_5H_3Br_2$ C *ipso*), 135.8 (Ph C *ipso*) 134.1 ($C_5H_3Br_2$ C *para*), 128.7 (Ph C *meta*), 128.3 (Ph C *para*), 127.6 (Ph C *ortho*), 127.2 ($C_5H_3Br_2$ C *ortho*), 123.7 (imidazolyl C5); 123.3 (imidazolyl C4), 122.8 ($C_5H_3Br_2$ C-Br), 53.99 (CH_2). Microanalysis: Found: C, 36.00; H, 2.35; N, 5.18% $C_{32}H_{24}AuBr_5N_4$ requires, C, 36.22; H, 2.28; N, 5.28%. HRMS (ESI^+): Calcd for $C_{32}H_{24}Br_4N_4Au$ [M-Br^+], m/z 976.8400. Found, *m/z* 976.8420. Crystals suitable for X-ray diffraction studies were grown by diffusion of vapours between diethyl ether and a solution of complex **13** in acetonitrile.

Cell culture reagents

Rosewell Park Memorial Institute (RPMI-1640) medium (with L-glutamine and sodium bicarbonate), fetal bovine serum (FBS), penicillin–streptomycin were obtained from Sigma Aldrich. Cell culture medium consists of RPMI-1640 medium (with L-glutamine and sodium bicarbonate) supplemented with 10% v/v FBS and 1% v/v penicillin–streptomycin.

Cells were dissociated during passaging using trypsin solution 0.05% in Hanks balanced salt solution (HBSS), and ethylenediaminetetraacetic acid EDTA, without calcium or magnesium (Hyclone GE Healthcare Life Sciences). MTT (3-(4,5-dimethylthiazol-2-yl)-2,5-diphenyltetrazolium bromide) was obtained from Thermo Fisher. Phosphate buffered saline (PBS) was obtained from Astral Scientific. Stock solutions (10 mM) of test compounds were prepared in DMSO (cell culture grade), obtained from Bio-Strategy. DMSO (to dissolve the MTT after incubation step in the MTT assay) was obtained from Sigma Aldrich.

Cell culture

Human ovarian cancer cells (OVCAR-8, from ATCC) were cultured in 75 cm^2 tissue culture flasks in cell culture medium (10 mL) at 37 °C under air (5% humidity, 5% CO_2). After being incubated for 2 days, the cells had reached ~ 80% confluency and were then passaged as follows. The medium was poured off, the cells were detached by incubation and agitation with trypsin (3 mL) for 3–5 min at 37 °C. To neutralise trypsin solution, cell culture medium (3 mL) was added, and the cell suspensions were transferred to Falcon tubes and centrifuged for 5 min at 1500 rpm. The supernatant was drawn off by pipette then cell pellet was resuspended in culture medium (10 mL). The cells were replated into three tissue culture flasks (2 mL cell suspension and 8 mL culture medium per flask) and incubated for two days. The cell culture medium was replaced after 1 day if the cells had shown substantial proliferation and confluency.

Cell viability assays

Stock solutions of Au-NHC compounds (10 mM) were prepared in DMSO and were stored at − 20 °C until required. These stock solutions were serially diluted in cell culture medium. For cell viability assays, OVCAR-8 cells that had reached 80% confluency in the tissue culture flasks were used. For cell seeding, the cells were dissociated as described above and cell number counted using a hemocytometer and suspended in culture medium at a final concentration of 2000 cells/100 µL.

Cell viability was determined using the MTT assay following the previously published protocol [38]. Briefly, OVCAR-8 cells were seeded in polystyrene 96-well plates (Costar; 2000 cells in 100 µL culture medium/well) and incubated for 24 h. Aliquots of solutions of Au-NHC compounds in cell culture medium (100 µL) were added to the wells so that the final concentrations of Au-NHC complex in wells was 0.39, 0.78, 1.56, 3.125, 6.25, 12.5, 25, 50, or 100 µM. The cells with the Au-NHCs were then incubated for 72 h. The medium was then carefully and completely removed by multichannel pipette and replaced by fresh cell culture medium (90 µL/well) and MTT solution (5 mg/mL MTT dissolved in PBS, 10 µL), and the plates were agitated to ensure homogeneity of solutions. The plates were incubated at 37 °C for 2 h, then the solution was removed by multichannel pipette and replaced by DMSO (200 µL/well) to solubilise the formazan purple colour from the live cells. The absorbance at 570 nm (A_{570}) was measured using a plate reader (Ensight Multimode Plate Reader, PerkinElmer). Relative cell viability (%) was determined by comparison of A_{570} for wells that had contained cells treated with Au-NHC complexes with A_{570} for wells that contained cells in culture medium alone. GraphPad Prism 8 software was used to determine IC_{50} values from cell viability data and to plot graphs of cell viability as a function of concentration of the Au-NHC complexes. Some imidazolium salts (precursors of NHC ligands) were used as negative controls for the cytotoxicity of the compounds to OVCAR-8 cells.

Conclusion

A number of Au-NHC complexes functionalised with 3,5-dibromophenyl substituents were synthesised. The syntheses were straightforward and their ^1H and ^{13}C NMR spectra were as expected. X-Ray diffraction showed that in the solid state, the intramolecular bond distances and bond angles were unexceptional, but the 3,5-dibromophenyl groups appear to exert significant intermolecular interactions. 3,5-Dibromphenyl groups were involved in intermolecular Br…π interactions with imidazolyl, phenyl

or 3,5-dibromophenyl groups, with Br…π distances in the range 3.6–4.7 Å. The 3,5-dibromophenyl-functionalised Au-NHC complexes showed potent activity against OVCAR-8 cells, and proved to be slightly more active than $[Au(Pr_2Im)_2]Br$ reported previously. We attribute the higher activity of the 3,5-dibromophenyl-functionalised complexes to their greater lipophilicity compared to $[Au(Pr_2Im)_2]Br$.

Supplementary Information The online version contains supplementary material available at https://doi.org/10.1007/s10847-021-01082-6.

Acknowledgements The authors acknowledge the facilities and the scientific and technical assistance of the Australian Microscopy & Microanalysis Research Facility at the Centre for Microscopy, Characterisation & Analysis, The University of Western Australia. Hawraa S. Al-Buthabhak thanks The Higher Committee for Education Development in Iraq (HCED) for financial support. Al-Salami is supported by the European Union's Horizon 2020 research and innovation programme under the Marie Skłodowska-Curie Grant Agreement No 872370. Al-Salami is also supported by Beijing Nat-Med Biotechnology Co., Ltd, and Glanis Biotech Ltd.

References

1. Modica-Napolitano, J.S., Weissig, V.: Treatment strategies that enhance the efficacy and selectivity of mitochondria-targeted anticancer agents. Int. J. Mol. Sci. **16**, 17394–17421 (2015). https://doi.org/10.3390/ijms160817394
2. Holmgren, A., Lu, J.: Thioredoxin and thioredoxin reductase: current research with special reference to human disease. Biochem. Biophys. Res. Commun. **396**, 120–124 (2010). https://doi.org/10.1016/j.bbrc.2010.03.083
3. Baker, A., Payne, C.M., Briehi, M.N., Powis, G.: Thioredoxin, a gene found overexpressed in human cancer, inhibits apoptosis in vitro and in vivo. Cancer Res. **57**, 5162–5167 (1997)
4. Berners-Price, S.J., Filipovska, A.: Gold compounds as therapeutic agents for human diseases. Metallomics **3**, 863 (2011). https://doi.org/10.1039/c1mt00062d
5. Modica-Napolitano, J.S., Aprille, J.R.: Delocalized lipophilic cations selectively target the mitochondria of carcinoma cells. Adv. Drug Deliv. Rev. **49**, 63–70 (2001)
6. Modica-Napolitano, J.S., Singh, K.K.: Mitochondria as targets for detection and treatment of cancer. Expert Rev. Mol. Med. **4**, 1 (2002). https://doi.org/10.1017/S1462399402004453
7. Rackham, O., Nichols, S.J., Leedman, P.J., Berners-Price, S.J., Filipovska, A.: A gold(I) phosphine complex selectively induces apoptosis in breast cancer cells: implications for anticancer therapeutics targeted to mitochondria. Biochem. Pharmacol. **74**, 992–1002 (2007). https://doi.org/10.1016/j.bcp.2007.07.022
8. Hickey, J.L., Ruhayel, R.A., Barnard, P.J., Baker, M.V., Berners-Price, S.J., Filipovska, A.: Mitochondria-targeted chemotherapeutics: the rational design of gold(I) N-heterocyclic carbene complexes that are selectively toxic to cancer cells and target protein selenols in preference to thiols. J. Am. Chem. Soc. **130**, 12570–11571 (2008). https://doi.org/10.1021/ja804027j
9. McKeage, M.J., Maharaj, L., Berners-Price, S.J.: Mechanisms of cytotoxicity and antitumor activity of gold(I) phosphine complexes: the possible role of mitochondria. Coord. Chem. Rev. **232**, 127–135 (2002)
10. McKeage, M.J., Berners-Price, S.J., Galettis, P., Bowen, R.J., Brouwer, W., Ding, L., Zhuang, L., Baguley, B.C.: Role of lipophilicity in determining cellular uptake and antitumour activity of gold phosphine complexes. Cancer Chemother. Pharmacol. **46**, 343–350 (2000)
11. Wedlock, L.E., Kilburn, M.R., Cliff, J.B., Filgueira, L., Saunders, M., Berners-Price, S.J.: Visualising gold inside tumour cells following treatment with an antitumour gold(I) complex. Metallomics **3**, 917–925 (2011). https://doi.org/10.1039/c1mt00053e
12. Berners-Price, S.J., Mirabelli, C.K., Johnson, R.K., Mattern, M.R., McCabe, F.L., Faucette, L.F., Sung, C.-M., Mong, S.M., Sadler, P.J., Crooke, S.T.: In vivo antitumor activity and in vitro cytotoxic properties of bis[1,2-bis(diphenylphosphino)ethane] gold(I) chloride. Cancer Res. **46**, 5486–5493 (1986)
13. Barnard, P.J., Baker, M.V., Berners-Price, S.J., Day, D.A.: Mitochondrial permeability transition induced by dinuclear gold(I)–carbene complexes: potential new antimitochondrial antitumour agents. J. Inorg. Biochem. **98**, 1642–1647 (2004). https://doi.org/10.1016/j.jinorgbio.2004.05.011
14. Zhang, C., Maddelein, M.L., Wai-Yin Sun, R., Gornitzka, H., Cuvillier, O., Hemmert, C.: Pharmacomodulation on gold-NHC complexes for anticancer applications—is lipophilicity the key point? Eur. J. Med. Chem. **157**, 320–332 (2018). https://doi.org/10.1016/j.ejmech.2018.07.070
15. Porchia, M., Pellei, M., Marinelli, M., Tisato, F., Del Bello, F., Santini, C.: New insights in Au-NHCs complexes as anticancer agents. Eur. J. Med. Chem. **146**, 709–746 (2018). https://doi.org/10.1016/j.ejmech.2018.01.065
16. Zou, T., Lum, C.T., Lok, C.N., Zhang, J.J., Che, C.M.: Chemical biology of anticancer gold(III) and gold(I) complexes. Chem. Soc. Rev. **44**, 8786–8801 (2015). https://doi.org/10.1039/c5cs00132c
17. Marzano, C., Gandin, V., Folda, A., Scutari, G., Bindoli, A., Rigobello, M.P.: Inhibition of thioredoxin reductase by auranofin induces apoptosis in cisplatin-resistant human ovarian cancer cell. Free Radic. Biol. Med. **42**, 872–881 (2007). https://doi.org/10.1016/j.freeradbiomed.2006.12.021
18. Hoke, G.D., Macia, R.A., Meunier, P.C., Bugelski, P.J., Mirabelli, C.K., Rush, G.F., Matthews, W.D.: In vivo and in vitro cardiotoxicity of a gold-containing antineoplastic drug candidate in rabbit. Toxicol. Appl. Pharmacol. **100**, 293–306 (1989)
19. Barnard, P.J., Wedlock, L.E., Baker, M.V., Berners-Price, S.J., Joyce, D.A., Skelton, B.W., Steer, J.H.: Luminescence studies of the intracellular distribution of a dinuclear gold(I) N-heterocyclic carbene complex. Angew. Chem. Int. Ed. Engl. **45**, 5966–5970 (2006). https://doi.org/10.1002/anie.200601526
20. Lu, Y., Liu, Y., Xu, Z., Li, H., Liu, H., Zhu, W.: Halogen bonding for rational drug design and new drug discovery. Expert Opin. Drug Discov. **7**, 375–383 (2012). https://doi.org/10.1517/17460441.2012.678829
21. Schilder, R.J., Hall, L., Monks, A., Handel, L.M., Forance, J.R., Ozols, R.F., Fojo, A.T., Hamilton, T.C.: Metallothionein gene expression and resistance to cisplatin in human ovarian cancer. Int. J. Cancer **45**, 416–422 (1990)
22. Domcke, S., Sinha, R., Levine, D.A., Sander, C., Schultz, N.: Evaluating cell lines as tumour models by comparison of genomic profiles. Nat. Commun. **4**, 2126 (2013). https://doi.org/10.1038/ncomms3126
23. Lindley, J., Mason, T.J., Lorimer, J.P.: Sonochemically enhanced Ullmann reactions. Ultrasonics **25**, 45–48 (1987)
24. Yong, F.F., Teo, Y.C., Tay, S.H., Tan, B.Y.H., Lim, K.H.: A ligand-free copper(I) oxide catalyzed strategy for the N-arylation of azoles in water. Tetrahedron Lett. **52**, 1161–1164 (2011). https://doi.org/10.1016/j.tetlet.2011.01.005
25. Collado, A., Gomez-Suarez, A., Martin, A.R., Slawin, A.M., Nolan, S.P.: Straight forward synthesis of [Au(NHC)X] (NHC = N-heterocyclic carbene, X = Cl, Br, I) complexes. Chem. Commun. **49**, 5541–5543 (2013). https://doi.org/10.1039/c3cc43076f

26. de Fremont, P., Singh, R., Stevens, E.D., Petersen, J.L., Nolan, S.P.: Synthesis, characterization and reactivity of N-heterocyclic carbene gold(III) complexes. Organometallics **26**, 1376–1385 (2007)
27. Starikova, O.V., Dolgushin, G.V., Larina, L.I., Ushakov, P.E., Komarova, T.N., Lopyrev, V.A.: Synthesis of 1,3-dialkylimidazolium and 1,3-dialkylbenzimidazolium salts. Russ. J. Org. Chem. **39**, 1467–1470 (2003)
28. Achar, G., Patil, S.A., Małecki, J.G., Budagumpi, S.: Coumarin-substituted 1,2,4-triazole-derived silver(I) and gold(I) complexes: synthesis, characterization and anticancer studies. New J. Chem. **43**, 1216–1229 (2019). https://doi.org/10.1039/c8nj02927j
29. Baker, M.V., Barnard, P.J., Berners-Price, S.J., Brayshaw, S.K., Hickey, J.L., Skelton, B.W., White, A.H.: Cationic, linear Au(I) N-heterocyclic carbene complexes: synthesis, structure and anti-mitochondrial activity. Dalton Trans. (2006). https://doi.org/10.1039/b602560a
30. Meyer, E.A., Castellano, R.K., Diederich, D.: Interactions with aromatic rings in chemical and biological recognition. Angew. Chem. Int. Ed. **42**, 1210–1250 (2003)
31. Mitra, D., Bankoti, N., Michael, D., Sekar, K., Row, T.N.G.: C-halogen…pi interactions in nucleic acids: a database study. J. Chem. Sci. (2020). https://doi.org/10.1007/s12039-020-01794-1
32. van der Bondi, A.: Waals volumes and radii. J. Phys. Chem. **68**, 441–451 (1964)
33. Hussaini, S.Y., Haque, R.A., Razali, M.R.: Recent progress in silver(I)-, gold(I)/(III)- and palladium(II)-N-heterocyclic carbene complexes: a review towards biological perspectives. J. Organomet. Chem. **882**, 96–111 (2019). https://doi.org/10.1016/j.jorganchem.2019.01.003
34. Schmidt, C., Karge, B., Bronstrup, M., Ott, I.: Gold(I) NHC complexes: antiproliferative activity, cellular uptake, inhibition of mammalian and bacterial thioredoxin reductases, and gram-positive directed antibacterial effects. Chem. Eur. J. **23**, 1869–1880 (2017). https://doi.org/10.1002/chem.201604512
35. Sheldrick, G.M.: Crystal structure refinement with SHELXL. Acta Crystallogr. C **71**, 3–8 (2015). https://doi.org/10.1107/S2053229614024218
36. Spek, A.L.: PLATON SQUEEZE: a tool for the calculation of the disordered solvent contribution to the calculated structure factors. Acta Crystallogr. C **71**, 9–18 (2015). https://doi.org/10.1107/S2053229614024929
37. Garnier, T., Sakly, R., Danel, M., Chassaing, S., Pale, P.: Chan–Lam-type C-N cross-coupling reactions under base- and ligand-free CuI-zeolite catalysis. Synthesis **49**, 1223–1230 (2017). https://doi.org/10.1055/s-0036-1588652
38. Mosmann, T.: Rapid colorimetric assay for cellular growth and survival: application to proliferation and cytotoxicity assays. J. Immunol. Methods **65**, 55–63 (1983)